PNAS BRIEF REPORT | NEUROSCIENCE

Mosaicism-independent mechanisms contribute to Pcdh19-related epilepsy and repetitive behaviors in *Xenopus*

Jugeon Park[a], Eunee Lee[a], Chul Hoon Kim[b], Jiyeon Ohk[a,1], and Hosung Jung[a,1]

Edited by Trudi Schüpbach, Princeton University, Princeton, NJ; received December 11, 2023; accepted April 5, 2024

Protocadherin19 (*PCDH19*)-related epilepsy syndrome is a rare disorder characterized by early-onset epilepsy, intellectual disability, and autistic behaviors. *PCDH19* is located on the X chromosome and encodes a calcium-dependent single-pass transmembrane protein, which regulates cell-to-cell adhesion through homophilic binding. In human, 90% of heterozygous females, containing *PCDH19* wild-type and mutant cells due to random X inactivation, are affected, whereas mutant males, containing only mutant cells, are typically not. The current view, the cellular interference, is that the altered interactions between wild-type and mutant cells during development, rather than loss of function itself, are responsible. However, studies using *Pcdh19* knockout mice showed that the complete loss of function also causes autism-like behaviors both in males and females, suggesting that other functions of PCDH19 may also contribute to pathogenesis. To address whether mosaicism is required for *PCDH19*-related epilepsy, we generated *Xenopus tropicalis* tadpoles with complete or mosaic loss of function by injecting antisense morpholino oligonucleotides into the blastomeres of neural lineage at different stages of development. We found that either mosaic or complete knockdown results in seizure-like behaviors, which could be rescued by antiseizure medication, and repetitive behaviors. Our results suggest that the loss of PCDH19 function itself, in addition to cellular interference, may also contribute to *PCDH19*-related epilepsy.

epilepsy in females with mental retardation | Dravet syndrome | mosaicism | autism spectrum disorder | seizure

PCDH19 is composed of six consecutive extracellular cadherin (EC) domains, a transmembrane region, and a cytoplasmic domain with a C-terminal tail. PCDH19 is highly expressed in the developing neuroepithelium, during which homophilic interaction between the EC domains regulates cell-to-cell adhesion (1). Indeed, most pathogenic mutations in human are located in the EC domain (2), particularly in the adhesive interface (3). Mutations in the *PCDH19* gene have been mostly found in female heterozygous patients with epilepsy, who often inherited the mutant gene-containing X chromosome from the asymptomatic father (2). This unusual pattern of inheritance is explained by the cellular interference theory, which posits that the coexistence of wild-type and mutant neuroepithelial cells in the developing female brain (due to random X inactivation) or mosaic males (4–6) interfere with normal homophilic adhesion causing clustering of like cells, abnormal brain development, and the disease.

However, there have been reports of autism-related behaviors (7, 8) and seizure activity (9) in complete knockout mice, suggesting that additional mechanisms may contribute to pathogenesis. *Xenopus* tadpoles are a unique model to investigate this possibility as the embryo develops by holoblastic divisions, during which the fate of each cell is well described, allowing complete or mosaic delivery of gene expression–altering reagents. In this study, we knocked down *pcdh19* gene expression in all or half of the cells of the central nervous system (CNS) and compared their phenotypes relevant to *PCDH19*-related epilepsy, using the previously established methods to model epilepsy and autism (10, 11).

Results

Experimental Strategy. At the eight-cell stage following three rounds of cleavage, the two dorsal animal blastomeres contribute to most of the CNS in the tadpole (12). Therefore, injecting morpholino (MO) oligonucleotides into these two blastomeres at this stage leads to knockdown of gene expression in most cells in the CNS of the tadpole (Fig. 1 *A*, *a*). On the other hand, injecting a half dose of the same reagent into one of their two daughter cells following an additional round of cleavage would result in the same degree of gene knockdown in half of the CNS cells in the tadpole since MO activities are restricted to the daughter cells (Fig. 1 *A*, *b*) (12). We used a *pcdh19* translation-blocking MO (pcMO) or control MO (coMO) and found that complete knockdown resulted in the normal-looking tadpole (Fig. 1 *B*, *a*)

Author affiliations: [a]Department of Anatomy, Graduate School of Medical Science, Brain Korea 21 Project, Yonsei University College of Medicine, Seoul 03722, Republic of Korea; and [b]Department of Pharmacology, Graduate School of Medical Science, Brain Korea 21 Project, Yonsei University College of Medicine, Seoul 03722, Republic of Korea

Author contributions: J.O. and H.J. designed research; J.P. performed research; J.O. and H.J. analyzed data; E.L. and C.H.K. gave inputs to the design of the experiments, the data, and manuscript; and J.O. and H.J. wrote the paper.

The authors declare no competing interest.

[1]To whom correspondence may be addressed. Email: jyeon1703@yonsei.ac.kr or hosungjung@yonsei.ac.kr.

This article contains supporting information online at https://www.pnas.org/lookup/suppl/doi:10.1073/pnas.2321388121/-/DCSupplemental.

Published May 15, 2024.

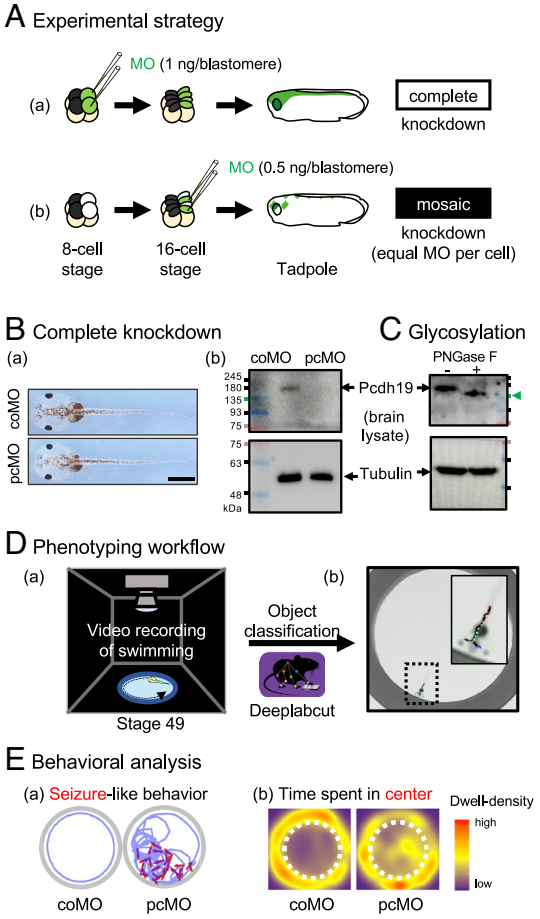

Fig. 1. Experimental strategy. (*A*) Microinjection strategy. (*a*) Complete knockdown. (*b*) Mosaic knockdown. (*B*) Efficiency of translation-blocking MO. (*a*) Normal gross morphology of stage 49 tadpoles injected with control (coMO) or *pcdh19* morpholino (pcMO). (Scale bar, 100 μm.) (*b*) Pcdh19 western blot from the brain. (*C*) Deglycosylation of Pcdh19 by PNGase F (arrowhead). (*D*) Trajectory analysis. (*a*) Video recording. (*b*) Pixel classification. (*E*) Phenotyping. (*a*) Seizure-like behaviors (red) in swimming trajectory (purple). (*b*) The center (dashed circle)-dwelling time visualized as a density plot.

with a level of Pcdh19 in the brain undetectable by western blot (Fig. 1 *B*, *b*). The Pcdh19 band migrated more slowly than expected for its calculated mass (~130 kDa) due to glycosylation (Fig. 1*C*). We analyzed the swimming behaviors of complete or mosaic knockdown tadpoles as previously described (10, 11) in a 2.5 cm arena for 10 min, extracted their poses using DeepLabCut trained with our dataset, and analyzed the swimming trajectory, swimming activity, and abrupt turning behaviors (Fig. 1*D*). One phenotype that we quantified is seizure-like behaviors (Fig. 1*E*, a, red arrow), characterized by intermittent bouts of rapid swimming, repetitive circling, lateral movement of the head with tremors, and/or C-shaped contractions (10, 11) (Movie S1). Another phenotype that we quantified is the time spent in the center of the arena (Fig. 1 *E*, *b*). As previously described (10), tadpoles tend to swim around the edge, whereas pcMO-injected tadpoles display short-ranged, repetitive circling behaviors in the center of the arena (dashed circle).

Histological Analysis of Complete and Mosaic *pcdh19* Knockdown in the Developing Brain. First, we asked whether cellular interference is observed in *Xenopus*. Complete and mosaic knockdown strategies delivered MO to approximately 96% and 50% of cells in the neuroepithelium, respectively (Fig. 2*A*). The distribution of GFP-positive cells showed clear difference depending on which MO was injected: pcMO-containing cells were segregated from noncontaining cells, in line with previous observations in mouse. We quantified this distribution by the k-nearest neighbors method: For every cell in the image, nine-nearest neighbors were selected forming a neighborhood composed of 10 cells, and the proportion of GFP^+ cells in the neighborhood was calculated (Fig. 2*B*). These values in the coMO group showed a bell-shaped distribution centered around 0.5. In contrast, those in the pcMO group showed two peaks around 0 and 1 (red arrows), indicating that GFP^+ and GFP^- cells segregate. This result also indicates that pcMO knocks down Pcdh19 proteins to a functionally significant degree. Both tissues were composed of similar proportions of GFP^+ cells (Fig. 2*C*), and the distribution, but not mean value, of GFP^+ cell proportions in neighborhoods was different (Fig. 2*D*). Therefore, cellular interference was observed in this *Xenopus* model.

Behavioral Phenotypes of Complete and Mosaic *pcdh19* Gene Knockdown. We compared seizure-like behaviors in tadpoles with complete or mosaic knockdown with their matching controls. Animals in both conditions showed a pcMO-dependent increase in seizure-like behaviors and the repetitive swimming activity in the center of the arena (Fig. 2*E*). These behaviors were rarely observed in coMO-injected tadpoles, and there was no difference between mosaic and complete *pcdh19* knockdown groups, suggesting that additional mechanisms other than the cellular interference contribute to seizure-like behaviors in *Xenopus*. Seizure-like behaviors of pcMO-injected tadpoles began to appear at premetamorphic stages with "adult-like" circuits (stages 47 to 49) but not in late embryonic stages (stages 43 to 45), as previously reported (10, 11) (Fig. 2*E*).

Relevance of Behaviors in Understanding *PCDH19*-related Epilepsy. If the seizure-like behavior induced by *pcdh19* knockdown in *Xenopus* represents epilepsy in human, antiseizure medication that can control seizures in patients with *PCDH19*-related epilepsy, such as potassium bromide (13), is expected to ameliorate it. To test this possibility, we selected the complete *pcdh19* knockdown tadpoles that displayed a high incidence of seizure-like behaviors and compared these behaviors before and after the treatment. We found that seizure-like behaviors, but not the center-dwelling tendency, were reduced in over 90% of tadpoles tested (Fig. 2*F*). These results indicate that *pcdh19* gene knockdown (complete or mosaic) in *Xenopus* produces two distinct behavioral phenotypes: seizure-like behaviors that can be prevented by antiseizure medications and repetitive behaviors that cannot be prevented.

Discussion

This is a direct and comprehensive comparison of littermate animals, in which *pcdh19* gene expression was knocked down in all or half of the cells in the brain. We found that both complete and mosaic knockdown induce similar degrees of behavioral abnormality: seizure-like and repetitive swimming behaviors. These behaviors occurred with or without cellular interference, suggesting that mechanisms other than the cellular interference contributed, in line with a recent finding of network hyperexcitability in *pcdh19* knockout zebrafish (14).

It is noteworthy that our findings contrast with cases in human, in which almost all nonmosaic male mutants are asymptomatic, with very few potential exceptions. We found that pcMO-dependent seizure-like behaviors appeared at premetamorphic stages, which suggests that they result from defects in Pcdh19-dependent synaptic refinements that occur during the preceding late embryonic stages. We speculate that synaptic refinements in human, which occur over a much longer duration than in model animals, are more resilient to perturbation. Therefore, cellular interference, which may influence global wiring patterns, is a main driver of pathogenesis in human, whereas both cellular interference and defective synaptic refinements contribute to pathogenesis in model animals.

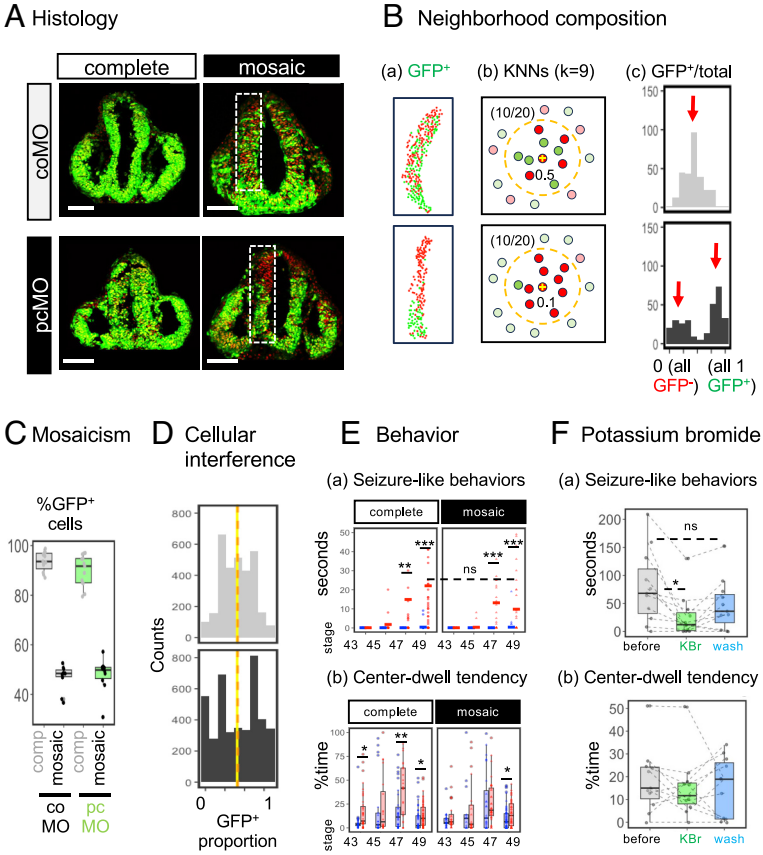

Fig. 2. Histological and behavioral outcomes of mosaic versus complete knockdown. (*A*) Representative images of GFP$^+$ (MO-containing) cells in the developing neuroepithelium (stage 27). Nuclei are counterstained in red. (Scale bars, 100 μm.) (*B*) Assessing the distribution of GFP$^+$ cells. (*a*) Cell counting. (*b*) K-nearest neighbors (KNNs). For each cell, a 10-cell neighborhood (k = 9, orange dashed circle) is defined and the GFP$^+$ proportion is calculated. In this example, 50% are GFP$^+$ in both conditions (i.e., 10/20), but the coMO and pcMO cells receive 0.5 and 0.1, respectively. (*c*) The distribution of neighborhood compositions. (*C*) Proportion of GFP$^+$ cells per brain. (*D*) Distribution of GFP$^+$ cells in all analyzed animals. The *y* axis represents the number of counted cells. $P < 2.2 \times 10^{-16}$ (D = 0.1408) in the asymptotic Kolmogorov–Smirnov test. Vertical lines represent means: coMO = 0.486 (yellow) and pcMO = 0.494 (orange), $P = 0.29$ in the unpaired *t* test. (*E*, *a*) Seizure-like behaviors (solid lines represent means) and (*b*) center-dwelling time of coMO (blue) and pcMO (red) tadpoles over time. Each point represents an observation (see *SI Appendix, Extended Materials and Methods* for the numbers of analyzed animals). *$P < 0.05$, **$P < 0.01$, ***$P < 0.001$, and ns, not significant; post hoc Tukey test following two-way ANOVA. (*F*) Effect of potassium bromide at stage 49. (a) Seizure-like behaviors. (b) Center-dwell tendency. *$P < 0.05$ and ns, not significant; repeated-measure ANOVA followed by post hoc Bonferroni tests (n = 11).

Abnormal synaptogenesis underlies neurodevelopmental diseases such as autism-spectrum disorders, in which apparent anatomical and cellular abnormalities are not seen in the brain. In this sense, it is intriguing that PCDH19 regulates the excitability of neurons (15). As the excitation–inhibition balance is established during development and its alteration is associated with autism spectrum disorders, we speculate that the loss of function in the *PCDH19* gene itself increases the vulnerability in developing a hyperactive neural network, the result of which may manifest as seizure-like and autism-like behaviors in *Xenopus* (this study), zebrafish (14), and mouse (8), but not often in human.

Materials and Methods

All the analyzed data were obtained from three or more independent experiments. *Xenopus* experiments were performed using the following morpholinos (OR, USA): pcMO, 5′-CCCTGCTCAGCCACAACCACATAGT-3′; coMO, 5′-CCTCTT ACCTCAGTTACAATTTATA-3′. Western blot analysis was performed using anti-PCDH19 (ab191198) or anti-Tubulin antibodies (ab6160) (Abcam) and PNGase F (P7367, Sigma-Aldrich). Data processing, visualization, and statistical analyses were performed using R (v4.3.0). Methods details are provided in *SI Appendix, Extended Materials and Methods*.

Data, Materials, and Software Availability. All study data are included in the article and/or supporting information.

ACKNOWLEDGMENTS. J.P. performed all experiments. J.O. and H.J. designed the experiments, analyzed the data, and wrote the paper with the help of all authors. E.L. and C.H.K. gave inputs to the design of the experiments, the data, and the manuscript. We thank Irene Cho and Nirali Anand for technical assistance. This work was supported by the National Research Foundation of Korea (NRF) grants funded by the Korean government (MSIT) (2017R1A2B4002683, 2018R1A5A2025079, and 2022M3E5E8018388 to H.J.; 2019R1A2C3002354 to C.H.K.) and the Ministry of Education (RS-2023-00247585 to J.O.).

1. D. T. Pederick *et al.*, Abnormal cell sorting underlies the unique X-linked inheritance of PCDH19 epilepsy. *Neuron* **97**, 59–66.e55 (2018).
2. C. Depienne *et al.*, Mutations and deletions in PCDH19 account for various familial or isolated epilepsies in females. *Hum. Mutat.* **32**, E1959–E1975 (2011).
3. S. R. Cooper, J. D. Jontes, M. Sotomayor, Structural determinants of adhesion by Protocadherin-19 and implications for its role in epilepsy. *Elife* **5**, e18529 (2016).
4. I. M. de Lange *et al.*, Male patients affected by mosaic PCDH19 mutations: Five new cases. *Neurogenetics* **18**, 147–153 (2017).
5. C. Depienne *et al.*, Sporadic infantile epileptic encephalopathy caused by mutations in PCDH19 resembles Dravet syndrome but mainly affects females. *PLoS Genet.* **5**, e1000381 (2009).
6. E. J. Romasko *et al.*, PCDH19-related epilepsy in a male with Klinefelter syndrome: Additional evidence supporting PCDH19 cellular interference disease mechanism. *Epilepsy Res.* **145**, 89–92 (2018).
7. S. Hayashi *et al.*, Loss of X-linked Protocadherin-19 differentially affects the behavior of heterozygous female and hemizygous male mice. *Sci. Rep.* **7**, 5801 (2017).
8. J. Lim, J. Ryu, S. Kang, H. J. Noh, C. H. Kim, Autism-like behaviors in male mice with a Pcdh19 deletion. *Mol. Brain* **12**, 95 (2019).
9. J. Rakotomamonjy, N. P. Sabetfakhri, S. L. McDermott, A. Guemez-Gamboa, Characterization of seizure susceptibility in Pcdh19 mice. *Epilepsia* **61**, 2313–2320 (2020).
10. K. G. Pratt, A. S. Khakhalin, Modeling human neurodevelopmental disorders in the Xenopus tadpole: From mechanisms to therapeutic targets. *Dis. Model Mech.* **6**, 1057–1065 (2013).
11. Y. Yoo *et al.*, GABBR2 mutations determine phenotype in rett syndrome and epileptic encephalopathy. *Ann. Neurol.* **82**, 466–478 (2017).
12. S. L. Nutt, O. J. Bronchain, K. O. Hartley, E. Amaya, Comparison of morpholino based translational inhibition during the development of Xenopus laevis and Xenopus tropicalis. *Genesis* **30**, 110–113 (2001).
13. J. Lotte *et al.*, Effectiveness of antiepileptic therapy in patients with PCDH19 mutations. *Seizure* **35**, 106–110 (2016).
14. B. K. Robens *et al.*, Mosaic and non-mosaic protocadherin 19 mutation leads to neuronal hyperexcitability in zebrafish. *Neurobiol. Dis.* **169**, 105738 (2022).
15. G. M. Serratto *et al.*, The epilepsy-related protein PCDH19 regulates tonic inhibition, GABA(A)R kinetics, and the intrinsic excitability of Hippocampal neurons. *Mol. Neurobiol.* **57**, 5336–5351 (2020).